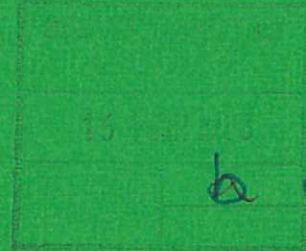




UKAEA

Report



METHANE FORMATION DURING DEUTERON
BOMBARDMENT OF CARBON IN THE
ENERGY RANGE OF 100 TO 1500 eV

K. SONE

CULHAM LABORATORY
Abingdon Oxfordshire

1982

© - UNITED KINGDOM ATOMIC ENERGY AUTHORITY - 1982
Enquiries about copyright and reproduction should be addressed to the
Librarian, UKAEA, Culham Laboratory, Abingdon, Oxon. OX14 3DB,
England.

METHANE FORMATION DURING DEUTERON BOMBARDMENT OF CARBON IN THE ENERGY RANGE OF 100 TO 1500 eV

K. SONE*

Culham Laboratory, Abingdon, Oxon OX14 3DB, UK
(Euratom/UKAEA Fusion Association)

November 1982

Abstract

Methane (CD_4) formation rates during deuteron bombardment of carbon (Papyex) have been measured in the energy range of 100 to 1500 eV. The temperature dependence of the methane formation rate is well explained by the model proposed by Erents et al. in the temperature range of 600 to 1150 K. The model, however, does not explain the dependence of the methane formation rate on the flux of incident deuterons at a certain temperature near T_m at which the formation rate has a maximum value. An alternative model is proposed in which the methane formation rate is assumed to be proportional to the product of the following three parameters: The surface concentration of deuterium atoms, the chemical reaction rate for the formation of methane, and the rate of production of vacancies on the surface by the deuteron bombardment. This model predicts an energy dependence of methane formation which has a maximum around 900 eV even at different deuteron fluxes, when the calculated result by Weissman and Sigmund is used for the surface deposited energy responsible for the production of vacancies.

* On leave from Japan Atomic Energy Research Institute,
Tokai-mura, Naka-gun, Ibaraki-ken, Japan

1. Introduction

Carbon is one of the promising materials for the first walls of controlled fusion devices. It has been considered one of the key surface material candidates in INTOR together with Be, BeO and SiC [1]. In spite of its advantageous characteristics such as high melting point and high thermal shock resistance as well as low-Z, it has some critical problems, for instance, chemical sputtering and reduction in thermal conductivity with irradiation. Here we are concerned with the chemical sputtering by low energy deuteron bombardment of carbon (Papyex).

Methane formation in carbon by hydrogen (H, D) exposure has been extensively studied using thermal atomic hydrogen [2-4,11,13,15] and ion beams in the energy range of 100 eV to 30 keV [5-10,12,14]. The measured data on methane formation yield with ion beams show a strong temperature dependence mostly having a maximum typically at 800 - 900 K. A model has been proposed by Erents et al. [7,9] to explain the temperature dependence. Although the model (hereafter we occasionally call it Erents' model for simplicity) is empirical, it has had considerable success. But the model is insufficient to explain the detailed energy dependence of the methane formation yield having a maximum in the vicinity of 1keV in the case of proton bombardment of pyrolytic graphite [12]. Recently, another model which has improved Erents' model by including surface deposited energy by energetic ion bombardment has been proposed by Yamada and Sone [16] to explain the energy dependence. In this paper the measured methane (CD₄) formation rates are analysed on the basis of these two models.

2. Experimental

The present experimental arrangement and measuring technique were similar to those previously used in deuteron re-emission and trapping experiments in carbon [18]. Deuteron bombardments were carried out by using a low energy accelerator. A D_2^+ ion beam was extracted from a hollow discharge type ion source followed by a Wien filter and Einzel lens. The acceleration voltage was determined by the potential applied to an extraction electrode. A stable beam current up to 4 μ A was obtained on a target at an acceleration voltage of between 100 V and 2500 V. Normally beam retardation applying a positive potential on the target was used for ion energies below 250 eV. The beam was well collimated to a 2 mm diameter spot on the target.

The target sample was a high purity flexible graphite ribbon known as Papyex (from Le Carbone), 30 mm \times 3 mm \times 0.1 mm. It was mounted between two insulated electrodes to provide a monitor of beam current, and to allow thermal desorption of all trapped deuterons and annealing of the sample by ohmic heating between bombardments. Target temperature was measured with a pyrometer directly through a window and a small hole in a chamber in which the target was placed. The target chamber was evacuated with a mercury diffusion pump and a titanium getter pump to an ultimate pressure of $\sim 1 \times 10^{-8}$ torr, and a pressure of $\sim 7 \times 10^{-8}$ torr with the beam on. Flow of D_2 gas from the ion source to the target chamber was minimised by two more mercury diffusion pumps used differentially at the ion source and in the beam line. Measurement of the methane (CD_4) released from the surface during bombardment was made with a quadrupole mass spectrometer by detecting continuously a mass 20 signal.

The present experiment involved measurements on temperature, flux and energy dependences of methane formation rates during deuteron bombardment. For the measurement on the temperature dependence of methane formation rates, the temperature was changed in turn from high to low temperatures to prevent an abrupt increase due to abrupt deuterium gas desorption when inversely changed. In the case of the measurement of the flux dependence of methane formation rates, the ion beam current was changed from 4 μA down to zero at constant target temperature. Concerning the measurement of the energy dependence of methane formation rates, the energy was decreased in turn from 1500 eV to 100 eV at definite fluxes and a constant target temperature. In these measurements the steady state levels were always taken as the values of the methane formation rates. Throughout the experiment all the measured values of the methane formation rates were relative and were not calibrated in absolute value.

3. Results and Discussion

A typical experimental result is shown in fig.1 of the temperature dependence of CD_4 formation rate at three different deuteron energies, 800 eV, 1250 eV and 1500 eV. Theoretical curves calculated from Erents' model [7,9] are also shown in the figure. Let us first review Erents' model briefly. If we neglect particle backscattering of energetic deuterons, the surface concentration of deuterium atoms n_s in the steady state situation is given by

$$n_s = \frac{J_0}{J_0\sigma + \tau^{-1}}, \quad \text{where } \tau = \tau_0 \exp(Q_2/RT) \quad (1)$$

where J_0 : incident deuteron flux,
 σ : detrapping cross section of D atoms induced by subsequently
incident deuterons.

We obtain the rate of formation of methane γ as:

$$\gamma = \frac{AJ_0 \exp(-Q_1/RT)}{J_0\sigma + \tau^{-1}}, \quad (2)$$

where $A \exp(-Q_1/RT)$ is the chemical reaction rate for the formation of methane as described in Erents' model, A being a constant. If we take account of the particle backscattering whose coefficient is denoted by B, eqs.(1) and (2) are changed into the following equations:

$$n_s = \frac{J_0(1-B)}{J_0(1-B)\sigma + \tau^{-1}}, \quad (3)$$

$$\gamma = \frac{AJ_0(1-B) \exp(-Q_1/RT)}{J_0(1-B)\sigma + \tau^{-1}}. \quad (4)$$

The theoretical curves in fig. 1 are calculated using eq.(4) by choosing suitable values of Q_1 , Q_2 and τ_0 . The backscattering coefficient B is taken from the energy dependence curve, fig.4. For the values of σ , we use the following empirical formula,

$$\sigma = \exp(-0.26625x^4 - 4.0417x^3 + 23.443x^2 - 62.138x + 22.953), \quad (5)$$

where $x = \log_{10} E$

where E is the incident deuteron energy in eV, and σ the detrapping cross section in cm^2 . Concerning how we have formulated eq. (5) we will describe later. The form of the peak temperature T_m at which

the methane formation rate has a maximum is given by

$$T_m = \frac{Q_2}{R} \left[\ln \frac{(Q_2/Q_1 - 1)}{J_0 (1-B) \sigma \tau_0} \right]^{-1}, \quad (6)$$

Erents' model can explain very well the temperature dependence of methane formation by choosing the fitting parameters $Q_1 = 23.0$ kcal/mole, $Q_2 = 51.5$ kcal/mole and $\tau_0 = 5.9 \times 10^{-11}$ s.

Figure 2 shows the methane formation rate at a constant temperature of 868 K as a function of deuteron beam current on the target. In spite of the fact that the temperature dependence is well explained by Erents' model, it does not explain the flux dependence of the methane formation rate since the curve calculated from the model (marked as $p = 0$ in Fig.2) passes through the points far from the experimental data. We have therefore improved Erents' model in the following way as has been proposed by Yamada and Sone [16].

Let us review the new model briefly. We assume that the surface concentration of the reactive sites of carbon for methane formation depends on the surface deposited energy, which produces vacancies and interstitials in the carbon lattice due to elastic collision cascades. This assumption is supported by recent experiments on hydrocarbon formation in the reaction of atomic hydrogen with pyrolytic graphite under simultaneous bombardment of atomic hydrogen and energetic ions [13,15]. An incident deuteron transfers energy to target atoms and this deposited energy results in the production of vacancies and interstitials, which can become the reactive sites for methane formation. The rate of production of the vacancies G may be proportional

to the product of the energy transfer $f_D(E)$ and the incident deuteron flux J_0 :

$$G \propto J_0 f_D(E) \quad (7)$$

As described by Damask [17], the time rates of change of vacancy concentrations are given for the two simplest mechanisms of vacancy loss as

$$dC_v/dt = G - \alpha \nu_v \lambda^2 C_v \quad (8)$$

for the limit of vacancies annealing to sinks, and

$$dC_v/dt = G - \nu_i C_v C_i \quad (9)$$

for the limit of recombination of vacancies and interstitials, where C_v , C_i and α are concentrations of vacancies, interstitials and sinks for vacancy loss, respectively, ν_v and ν_i are jump frequencies of vacancies and interstitials, respectively, and λ is the jump distance. The solutions for the vacancy concentrations in the steady state are

$$C_v = G/\alpha \nu_v \lambda^2 \quad , \quad (10)$$

and

$$C_v = (G/\nu_i)^{1/2} \quad , \quad (11)$$

for the two limits mentioned above. Since it is reasonable to consider that the real C_v exists between the two limits, we assume that the C_v is proportional to $(G/\nu)^p$ ($1/2 \leq p \leq 1$), where ν is the apparent jump frequency given by $\nu = \nu_0 \exp(-Q_3/RT)$. Therefore if we take the surface deposited energy into account, the methane formation rate γ is given by

$$\begin{aligned} \gamma &= S J_0 = A' G^p n_s \exp(-Q_1 RT) \\ &= A' (J_0 f_D / \nu_0)^p \frac{J_0 (1-B) \exp(-Q_1^+/RT)}{J_0 (1-B) \sigma + \tau^{-1}} \quad , \quad (12) \end{aligned}$$

where $Q_1^+ = Q_1 - pQ_3$, S is the methane formation yield per incident D atom, and A' a new proportionality constant. From eq.(12) we obtain S :

$$S = A' (J_0 f_D / \nu_0)^P \frac{(1-B) \exp(-Q_1^+ / RT)}{J_0 (1-B) \sigma + \tau^{-1}} \quad (13)$$

By differentiating eq.(12) with respect to T , the peak temperature T_m is given by

$$T_m = \frac{Q_2}{R} \left[\ln \frac{(Q_2 / Q_1^+ - 1)^{-1}}{J_0 (1-B) \sigma \tau_0} \right] \quad (14)$$

since $A' (J_0 f_D / \nu_0)^P$ in eq.(12) is independent of the temperature T . If we compare eq.(4) with eq.(12), we find that the two following replacements give a same formula: a) A in eq.(4) \longleftrightarrow $A' (J_0 f_D / \nu_0)^P$ in eq.(12), and b) Q_1 in eq.(4) \longleftrightarrow Q_1^+ in eq.(12). The situation is the same for eqs.(6) and (14) between Q_1 and Q_1^+ . It should be noted from this that if the same value of 23.0 kcal/mole is given to both Q_1 in Erents' model and Q_1^+ in the proposed model a common temperature dependence curve calculated by the two models at a given energy is obtained, since the factors A and $A' (J_0 f_D / \nu_0)^P$ are independent of the temperature T . This is the reason why we write as " $Q_1, Q_1^+ = 23.0$ kcal/mol" in fig. 1.

It is obvious from eq.(12) that if we neglect the term $(J_0 f_D / \nu_0)^P$, that is, if we give the parameter p zero value, we obtain the same equation as eq.(4). Instead of $p = 0$, the value of $p = 0.6$ gives the best fit to the experimental flux dependence as shown in fig. 2. For the first four experimental data points from $4.0 \mu A$ to $3.4 \mu A$, the methane formation rate has a much lower value than the calculated curve for $p = 0.6$. This is probably due to the experimental procedure since the order of measuring the data points is from high ($4 \mu A$)

to low beam current, which could result in the surface damage concentrations not having reached equilibrium. As evidence for this, the value for the second measurement at a high fluence is higher than the first one at 4 μA . We have also made such measurements for deuteron energies of 1000 eV and 1250 eV, in which similar results to fig.2 were obtained. From these results we conclude that we have to consider surface damage concentrations produced by energetic deuteron bombardment.

As the next step we have measured the methane formation rate at different energies from 1500 eV down to 100 eV at a constant temperature of 868 K. By obtaining a value for the normalisation constant A' by fitting the cross section data obtained previously [18] at 1000 eV, we can determine from the relative intensities of the CD_4 signal of the quadrupole mass spectrometer the detrapping cross section σ as a function of deuteron energy. The result is shown in fig.3, which indicates that very good agreement between the present data and the previous results is obtained except in the low energy region around 100 eV. For convenience of numerical calculations we have made an empirical formula giving the value of σ as a function of E by least square fitting, which results in the form of eq.(5). The empirical formula can extend to the higher energy region near 20 keV.

In fig.4 are shown the surface deposited energy f_D and the back-scattering coefficient B used here both as a function of energy. As for the surface deposited energy $f_D(E)$, theoretical results by Weissman and Sigmund [23] are used. The Monte Carlo results for $f_D(E)$ by Haggmark and Wilson [24] have also been tried, but this gives poor agreement of calculated cross sections with the previous experimental data [18]. The following explanation is possible. Equation (12) is re-formed to give σ by

$$\sigma = \frac{1}{J_0(1-B)\gamma} \{A' J_0(1-B) \exp(-Q_1^+/RT) (J_0 f_D / v_0)^P - \gamma/\tau\} \quad (15)$$

The Monte Carlo result by Haggmark and Wilson gives a recoil energy density in the outward direction, f_D^{outward} , when we define three different regions for the direction of the recoiling atoms by dividing the full solid angle into three equal parts, i.e. the outward, sideward and inward directions (as Behrisch et al. have done using the MARLOWE code [25]). However, for the analysis of methane formation we should take the total recoil energy density f_D^{total} which is equal to $f_D^{\text{outward}} + f_D^{\text{sideward}} + f_D^{\text{inward}}$, because all recoils should be responsible for the formation of reactive sites. Thus it is natural that the results of Weissman and Sigmund [23] give better agreement than those of Haggmark and Wilson [24]. The f_D in eq.(15) decreases with decreasing energy E below 500 eV in the results of Haggmark and Wilson, while it increases with decreasing E in that energy region in the results of Weissman and Sigmund. The former results in an underestimate in σ by nearly 100% with respect to the previous data of σ [18]. For this reason we do not take the Monte Carlo results for $f_D(E)$.

Figure 5 shows the calculated methane formation yield per incident D atom at the peak temperature T_m given in eq.(6) at different deuteron fluxes as a function of deuteron energy E . The following results are obtained from fig.5:

1. There is a pronounced energy dependence in methane formation yield S per incident D atom. At 900 eV the value of S has a sharp maximum at any deuteron flux.
2. The yield at a given energy increases with increasing deuteron flux.

The conclusion (1) is roughly supported by the results for hydrogen chemical sputtering [12,16].

Conclusions

The measurements of methane formation rates during deuteron bombardment of carbon (Papyex) have been made as a function of temperature, flux and energy. The results are summarised as follows.

1. The temperature dependence is well explained by Erents' model in the temperature range of between 600 K and 1150 K.
2. Erents' model cannot explain the flux dependence. It is explained by an alternative model in which the methane formation rate is assumed to be proportional to the product of the three parameters: the surface concentration of deuterium atoms, the chemical reaction rate for the formation of methane and the rate of production of vacancies on the surface by the deuteron bombardment.
3. The detrapping cross sections as a function of energy have been calculated using the measured relative intensities of methane released at different energies and the calculated result of surface deposited energy by Weissmann and Sigmund. The model including the detrapping cross sections thus calculated predicts an energy dependence of methane formation rate which has a maximum around 900 eV over a range of different deuteron fluxes.

Acknowledgments

The author would like to thank S K Erents and J Vince for their kind help and useful comments during the experiment. He is grateful to R Yamada (JAERI) and G M McCracken for fruitful discussion on the energy dependence problem, and to the Science and Technology Agency of Japan and Japan Atomic Energy Research Institute for financial support.

References

- [1] M. Abdou, N. Fujisawa, M. Harrison, T. Hiraoka, V. Pistunovich, P. Schiller, J. Schmidt, G. Shatalov and D. Smith, Impurity Control, Report of Group B, INTOR Phase IIA Session V, July 1982.
- [2] B. J. Wood and H. Wise, J. Phys. Chem., 73 (1969) 1348.
- [3] R. K. Gould, J. Chem. Phys., 63 (1975) 1825.
- [4] M. Balooch and D. R. Olander, *ibid*, p.4772.
- [5] J. Roth, J. Bohdansky, W. Poschenrieder and M. Sinha, J. Nucl. Mater., 63 (1976) 222.
- [6] N. P. Busharov, E. A. Gorbatov, V. M. Gusev, M. I. Guseva and Y. V. Martynenko, *ibid*, p.230.
- [7] S. K. Erents, C. Braganza and G. M. McCracken, *ibid*, p.399.
- [8] K. Sone, H. Ohtsuka, T. Abe, R. Yamada, K. Obara, O. Tsukakoshi, T. Narusawa, T. Satake, M. Mizuno and S. Komiya, Proc. Intern. Symp. on Plasma Wall Interaction, Julich, 1976 (Pergamon Press, 1977) p.323.
- [9] C. M. Braganza, S. K. Erents and G. M. McCracken, J. Nucl. Mater., 75 (1978) 220.
- [10] J. N. Smith Jr. and C. H. Meyer Jr., *ibid*, 76 & 77 (1978) 193.
- [11] T. Abe, K. Obara and Y. Murakami, *ibid*, 91 (1980) 223.
- [12] R. Yamada, K. Nakamura, K. Sone and M. Saidoh, *ibid*, 95 (1980) 278.
- [13] R. Yamada, K. Nakamura and M. Saidoh, *ibid*, 98 (1981) 167.
- [14] J. Roth, J. Bohdansky and K. L. Wilson, J. Nucl. Mater., 111 & 112 (1982) 775.
- [15] E. Vietzke, K. Flaskamp and V. Philipps, *ibid*, 763.
- [16] R. Yamada and K. Sone (submitted to J. Nucl. Mater.).

- [17] A. C. Damask, in "Studies in Radiation Effects in Solids" Vol.2, ed. G. J. Dienes (Gordon and Breach Sci. Pub., New York, 1977) p.1.
- [18] K. Sone and G. M. McCracken, J. Nucl. Mater., 111 & 112 (1982), 606.
- [19] B. M. U. Scherzer, R. Behrisch, W. Eckstein, U. Littmark, J. Roth and M. K. Sinha, J. Nucl. Mater., 63 (1976) 100.
- [20] G. Staudenmaier, J. Roth, R. Behrisch, J. Bohdanský, W. Eckstein, P. Staib, S. Matteson and S. K. Erents, *ibid*, 84 (1979) 149.
- [21] S. K. Erents, Nucl. Instrum. Methods, 170 (1980) 455.
- [22] T. Tabata, R. Ito, K. Morita and Y. Itikawa, Jap. J. Appl. Phys., 20 (1981) 1929.
- [23] R. Weissman and P. Sigmund, Radiation Effects, 19 (1973) 7.
- [24] L.G. Haggmark and W. D. Wilson, J. Nucl. Mater., 76 & 77 (1978) 149.
- [25] R. Behrisch, G. Mederlechner, B.M.U. Scherzer and M.T. Robinson, Appl. Phys., 18 (1979) 391.

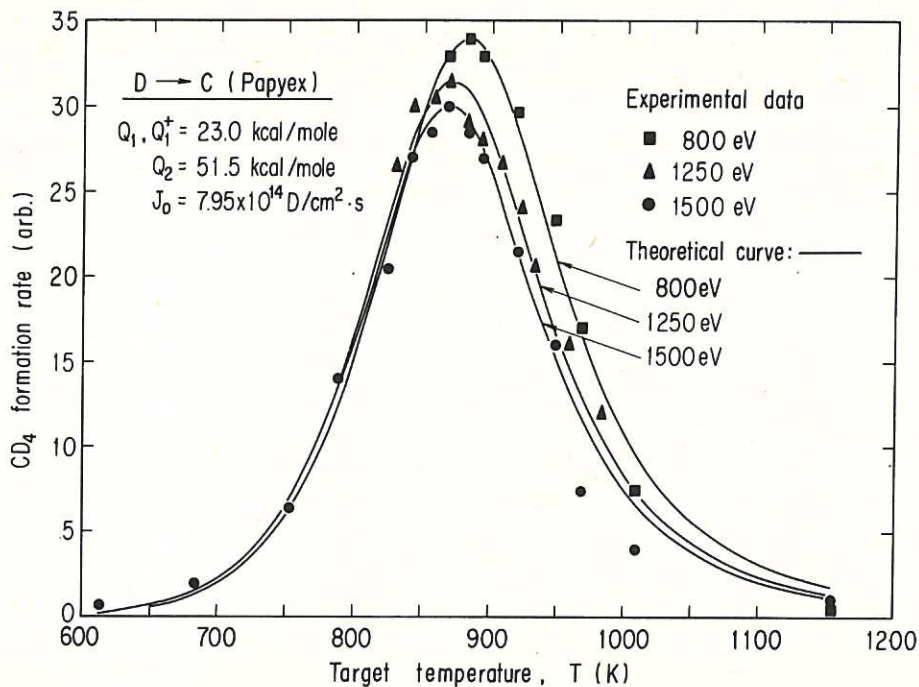


Fig.1 Steady state methane release rate from a Papyex carbon surface during bombardment by deuterons at different energies and temperatures. Incident deuteron flux: $J_0 = 7.95 \times 10^{14} \text{ D/cm}^2 \cdot \text{s}$. Theoretical curves are shown together with experimental data, where each theoretical maximum coincides with the corresponding experimental maximum. For the activation energies Q_1 , Q_1^\dagger and Q_2 , see text.

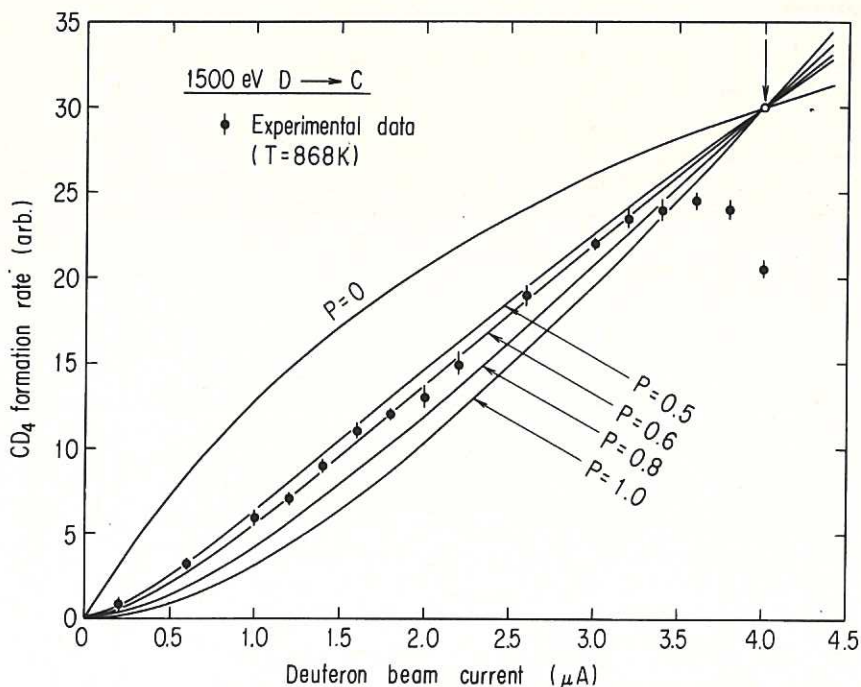


Fig.2 Methane release rate from a Papyex carbon surface during deuteron bombardment as a function of deuteron beam current. The values of the deuteron beam current (in μA) are for a 2mm diameter beam spot on the target. Surface temperature: 868K. Deuteron energy: 1500eV. Theoretical curves are also given for different values of a damage parameter p (see text). They are adjusted to pass through the point (4.0 μA , 30.0), which corresponds to the maximum of the temperature dependence curve, fig.1. The order of measuring the data points is from high (4 μA) to low beam current.

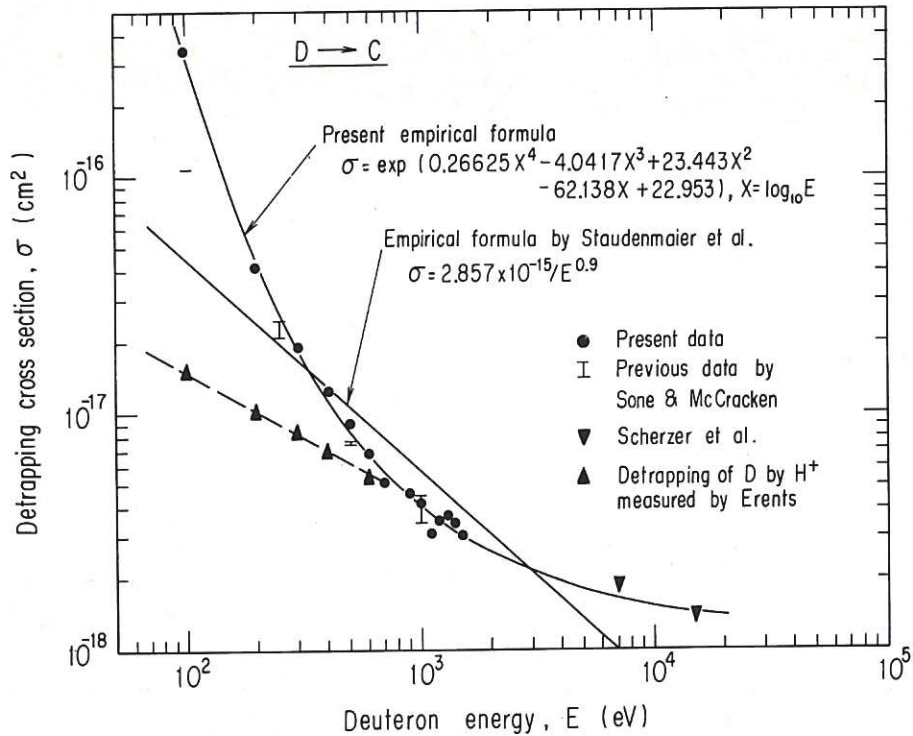


Fig.3 Detraping cross section versus deuteron energy. The present empirical formula has been derived by least square fitting to the present experimental data and the data by Scherzer et al [19]. Experimental data obtained previously by re-emission measurement at room temperature [18], another empirical formula by Staudenmaier et al [20] and detraping of D by proton bombardment measured by Erents [21] are also plotted for comparison.

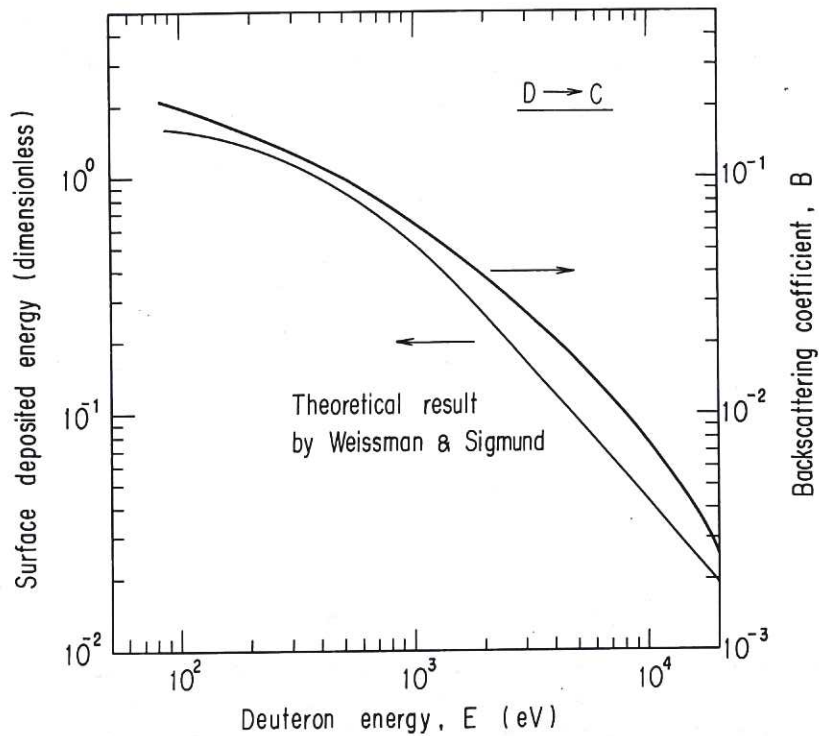


Fig.4 Surface deposited energy (dimensionless) predicted from the theory of Weissman and Sigmund [23], and backscattering coefficient, both as a function of deuteron energy. The backscattering coefficient curve is composed by combining the data compiled by Staudenmaier et al [20] ($E \lesssim 1000$ eV) and the data empirically predicted by Tabata et al [22] ($E \gtrsim 20$ keV).

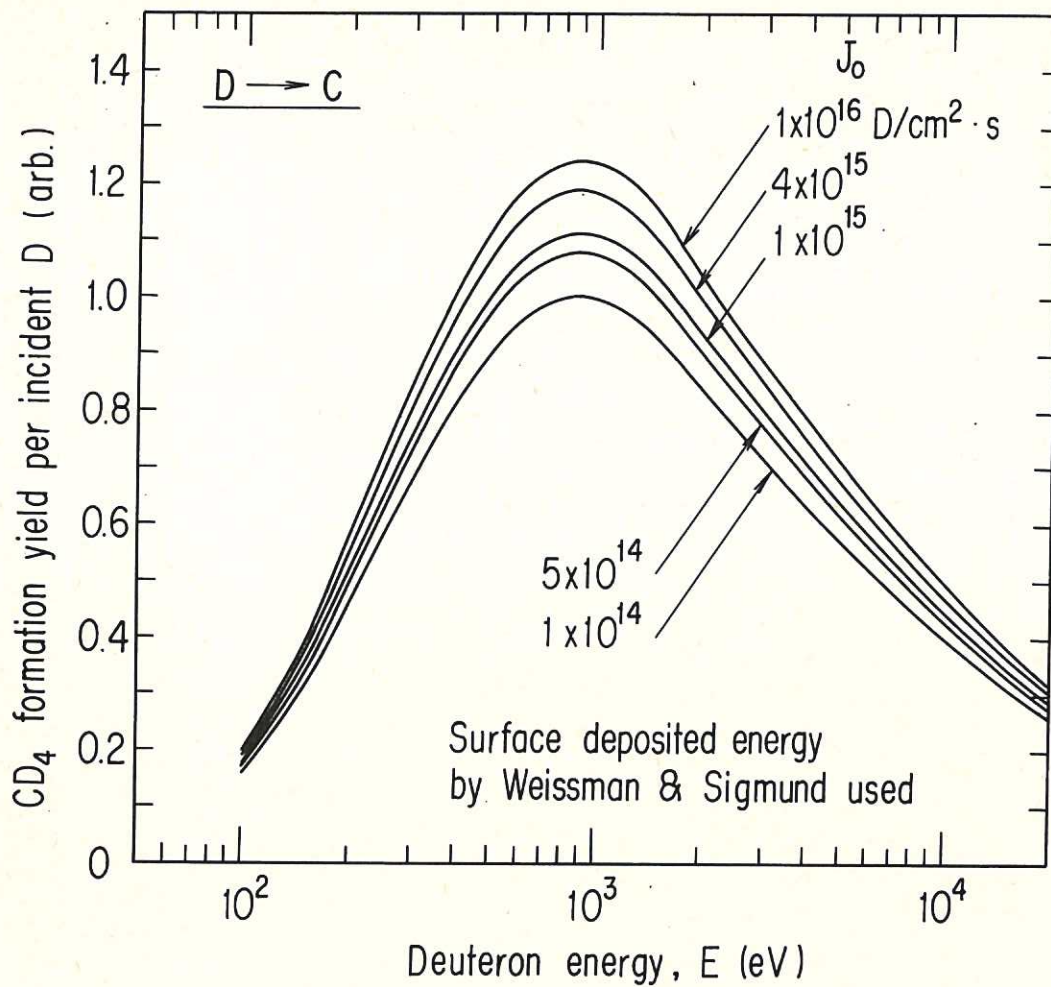


Fig.5 Calculated energy dependence of methane formation yield per incident D atom at the peak temperature T_m at different deuteron fluxes. The relative intensities of the formation yield are normalised at the point (900eV, 1×10^{14} D/cm²s).

The first part of the document discusses the importance of maintaining accurate records of all transactions. It emphasizes that every entry, no matter how small, should be recorded to ensure the integrity of the financial statements. This includes not only sales and purchases but also expenses, income, and any other financial activity.

The second part of the document provides a detailed explanation of the accounting cycle. It outlines the ten steps involved in the process, from identifying the accounting entity to preparing financial statements. Each step is explained in detail, with examples provided to illustrate the concepts.

The third part of the document discusses the various types of accounts used in accounting. It explains the difference between assets, liabilities, and equity accounts, and how they are classified. It also discusses the importance of understanding the normal balances for each type of account.

The fourth part of the document provides a comprehensive overview of the accounting equation. It explains how the equation is used to verify the accuracy of the accounting records and how it can be used to determine the missing value in an account.

The fifth part of the document discusses the importance of adjusting entries. It explains how these entries are used to ensure that the financial statements reflect the true financial position of the company at the end of the accounting period.

The sixth part of the document provides a detailed explanation of the closing process. It outlines the steps involved in closing the temporary accounts and transferring their balances to the permanent accounts.

The seventh part of the document discusses the importance of maintaining accurate records of all transactions. It emphasizes that every entry, no matter how small, should be recorded to ensure the integrity of the financial statements.

The eighth part of the document provides a detailed explanation of the accounting cycle. It outlines the ten steps involved in the process, from identifying the accounting entity to preparing financial statements.

The ninth part of the document discusses the various types of accounts used in accounting. It explains the difference between assets, liabilities, and equity accounts, and how they are classified.

The tenth part of the document provides a comprehensive overview of the accounting equation. It explains how the equation is used to verify the accuracy of the accounting records and how it can be used to determine the missing value in an account.

HER MAJESTY'S STATIONERY OFFICE

Government Bookshops

49 High Holborn, London WC1V 6HB
(London post orders: PO Box 569, London SC1 9NH)

13a Castle Street, Edinburgh EH2 3AR

41 The Hayes, Cardiff CF1 1JW

Brazennose Street, Manchester M60 8AS

Southey House, Wine Street, Bristol BS1 2BQ

258 Broad Street, Birmingham B1 2HE

80 Chichester Street, Belfast BT1 4JY

Publications may also be ordered through any bookseller